Trends and Variability of Snow Water Equivalent in the Northern Hemisphere

Hester Scheepers, Thian Yew Gan

Dept. Of Civil and Environmental Engineering, University of Alberta, Edmonton, AB

FloodNet Annual General Meeting
Montreal, 27th to 28th June 2017

Introduction

Snowpacks are important because they store water that is later released into soil and rivers. In many parts of the world, snow accumulation is a major source of water for irrigation, hydro-electrical generation and drinking water. Most Canadian river basins are covered with snow in the winter which are dominated by snowmelt runoff in the spring. Under global warming conditions snow cover and snow depth are expected to change. Satellite measurements enables research into global snow accumulation patterns. The objective of this study is to identify the trends and variability of snow water equivalent (SWE), that is, the depth liquid water that would result if the snowpack melted, of the Northern Hemisphere.

Methodology

GlobSnow SWE Data:
SWE data was obtained from the GlobSnow-2 SWE product which is based on a combination of satellite and ground-based synoptic weather station data. Daily SWE data was extracted for 1 November to 31 March between 1988 and 2016. Each year was divided into 30 pentads (five-day averages). "P1" represents the average SWE for pentad 1 (1-5 November), while "P30" is the average SWE for 26-30 March.

ERA-Interim Data
This study made use of the surface temperature and snowfall variables from the ERA-Interim reanalysis dataset, which represents a third generation reanalysis and is the latest global atmospheric reanalysis produced by ECMWF.

Climate Indices:
Monthly climate indices used in this study included the Artic Oscillation (AO), North Atlantic Oscillation (NAO), Pacific North American pattern (PNA), Pacific Decadal Oscillation (PDO), Southern Oscillation Index (SOI) and the Niño3 index.

Trends:
Trends and trend magnitude in SWE, temperature and snowfall data was tested using the non-parametric, Mann-Kendall test (Kendall, 1975; Mann, 1945) and the Theil–Sen slope estimator (Sen, 1968). which can handle non-normality, missing values, and seasonality.

Principle Component Analysis:
Principal component analysis (PCA) is a method to reduce the dimensionality of data while retaining the variability through an orthogonal transformation which identifies the principle components (PCs) along which the variation is maximal. The leading PCs were correlated with the various climate indices.

Self-Organizing Map:
The self-organizing map (SOM) (Kohonen, 2001) is a type of artificial neural network which aims to discover an underlying structure in the data through unsupervised learning to produce a two dimensional array of nodes, called a map, that are organized in such a way that similar items are close together.

For each grid in the Northern Hemisphesre with SWE data, a niveograph was available for the 28 years in the study period, which was used input for the SOM analyses. This resulted in 20 artificial niveographs to which all the input niveographs could be matched, named cluster 1 to cluster 20.

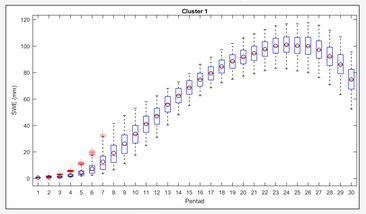

Figure 1: Boxplots of SWE for all grids assigned to cluster 1 between 1988 – 2016.

Cluster 1 is represented in boxplot form in Figure 1. The sum of the mean SWE for each of the 30 pentads represented the area under the niveograph of SWE for a specific cluster. This allowed each of the 20 clusters to be represented by a single value which was correlated to climate indices.

Results

Trend:
The SWE and accumulated snowfall trends were calculated for each pentad (1-30) individually using the non-parametric Mann-Kendall test at 0.05 significant level, shown in Figure 2a and 2b. Pentad trends for six consecutive pentads are plotted together such that an estimate of each month is portrayed in a single plot. Pixels that exhibited significant increasing trends are shown in the red colour range, while significant decreasing trends are shown in the blue colour range.

Significant decreasing trends are located in North America;: over most of Baffin Island in Nunavut, Canada; The northern tip of Quebec (around 58°N); in the North West Territories, north of Great Bear Lake; and some areas of Alaska. Some of the northern areas of Norway depict negative trends, as well as small areas in the Netets Autonomous Okrug, Russia, Komi Republic, Russia. and in the region of Mongolia. Increasing trends are evident in eastern Russia on the coast of Khabarovsk Krai, Russia along the Dzhugdzhur Range, in Sakha Republic, and Magadan, Russia.

SWE was correlated to accumulated snowfall (Figure 2c) and temperature (Figure 2d) for each pentad. Significant positive correlations are shown in the red colour range, while significant negative correlations are given in the blue colour range. Both temperature and accumulated snowfall are significantly correlated to SWE in most areas of the Northern Hemisphere, but accumulated snowfall appears more closely aligned with the location of decreasing SWE trends.

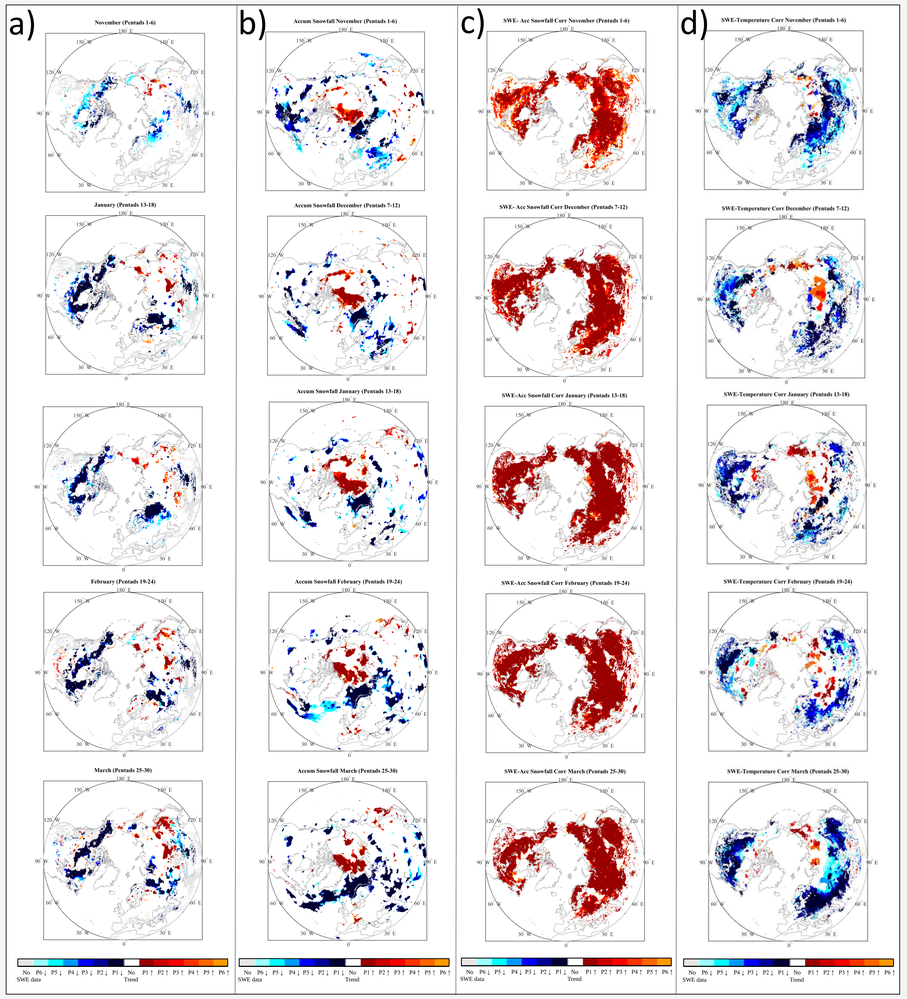

Figure 2. a) Northern Hemisphere increasing (red) and decreasing (blue) SWE pentad trends statistically significant at the 0.05 level. b) Accumulated snowfall trends. c) Correlation between SWE and accumulated snowfall. d) Correlation between SWE and temperature.

SWE variation:
The SOM analysis resulted in 20 clusters representing SWE niveographs. Figure 3 shows the frequency that each cluster type occurred for each grid over the study period. Blue regions represent areas with little inter-annual variability, while red regions exhibit large variation.

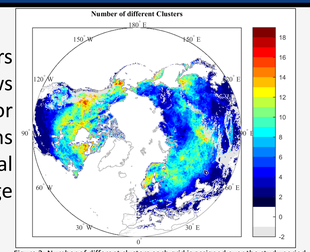

Figure 3: Number of different clusters each grid is assigned over the study period

For each grid in the Northern Hemisphere, the data for the 30 pentads in all 28 seasons was used to perform PCA. The score of the first principle component was correlated to the NDJFM climate index for each grid. Figure 4 shows the correlation between PC1 and the AO and the PNA.

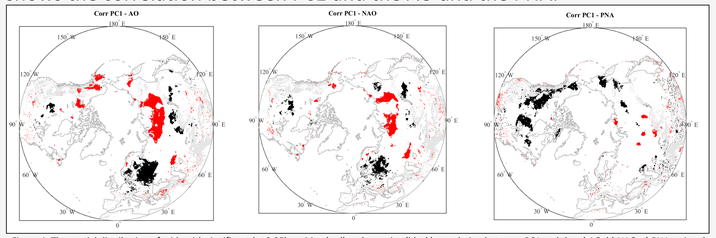

Figure 4: The spatial distribution of grids with significant (p<0.05) positive (red) and negative (black) correlation between PC1 and the a) AO, b) NAO, c) PNA, using the Spearman's rank correlation.

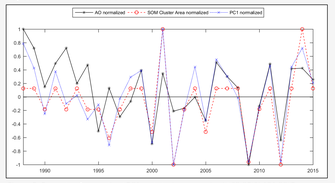

Figure 5: Example of normalized PC1 and cluster areas at grid 63.35°N 121.38°E compared with AO index (positive correlation)

Figure 5 shows the time series of the AO compared to normalised values of PC1 and the SOM cluster area for a single grid. This shows how the two different methods yield comparable results to investigate the inter-annual variability of SWE.

Conclusions

- There are more snow covered pixels that show statistically significant decreasing trends compared to increasing trends during throughout the season. Most of the increasing SWE trends are located in Asia. Most of the decreasing trends are geographically located north of 55° latitude, and are predominantly in Canada and European Russia..
- The median trend magnitudes detected for November to March range from -0.23 to -0.31 mm/yr, which could mean a reduction of snow depth of approximately 2.6 to 3.5 cm in 28 years assuming a snowpack density of 250 kg/m^3, which can impact relying on spring snowmelt for water supply.
- SWE is significantly correlated to both temperature and accumulated snowfall. The regions in Canada with significant decreasing SWE trends do not however correspond directly to the pixels that are correlated with temperature, suggesting that snowfall may have a larger influence on the observed SWE trends than temperature.
- Some climate anomalies could contribute to the inter-annual variability of SWE (The AO, NAO, and PNA). The PDO, SOI and Niño3 index showed comparably smaller areas that were significantly correlated. The SOM method and PCA yielded similar results to investigate the inter-annual variability of SWE.

References

Kendall, M. G. (1975), Rank Correlation Methods, Charles Griffin, London.

Kohonen, T. (2014), MATLAB Implementations and Applications of the Self-Organizing Map. Unigrafia Oy, Helsinki, Finland.

Mann, H. B. (1945), Nonparametric tests against trend, Econometrica, 13, 245–259.

Sen, P. K., 1968, Estimates of the regression coefficient based on Kendall's tau, J. Am. Stat. Assoc., 63, 1379-1389.